



Effect of Concentration on Morphological, Optical and Electrical Properties of Copper Doped Zinc Oxide Thin Films Deposited by Electrostatic Spray Pyrolysis (ESP) Technique

D. O. Samson^{1,2*} and E. K. Makama^{2,3}

¹Department of Physics, University of Abuja, P.M.B 117, Abuja, Nigeria.

²School of Physics, Universiti Sains Malaysia, 11800 USM, Gelugor, Penang, Malaysia.

³Department of Physics, University of Jos, P.M.B. 2084, Nigeria.

Authors' contributions

This work was carried out in collaboration between both authors. Author DOS designed the study, performed the statistical analysis, wrote the protocol and wrote the first draft of the manuscript. Authors DOS and EKM managed the analyses of the study. Authors DOS and EKM managed the literature searches. Both authors read and approved the final manuscript.

Article Information

DOI: 10.9734/JMSRR/2018/44271

Editor(s):

(1) Dr. Mehmet Cavas, Associate Professor, Department of Mechatronics Engineering, Firat University Faculty of Technology, Elazig, Turkey.

Reviewers:

(1) Ikhioya I. Lucky, University of Nigeria, Nigeria.

(2) En-Chih Chang, I-Shou University, Taiwan, R.O.C.

Complete Peer review History: <http://www.sciencedomain.org/review-history/27355>

Original Research Article

Received 31 August 2018

Accepted 13 November 2018

Published 22 November 2018

ABSTRACT

Pure zinc oxide (ZnO) and copper (Cu) doped ZnO thin films were synthesised from the precursor's concentrations (zinc acetate and copper acetate) onto glass substrate via spray pyrolysis deposition technique at 350°C in air ambient with different Cu doping concentrations (0%, 5%, 10%, 15% and 20%). The thin films were analysed with regards to its morphological, optical, and electrical properties before and after annealing. The results indicate that the annealing of the thin films leads to improved surface morphology and better crystallinity quality. Nanofibers were observed around the nucleation centre in the pure ZnO thin films. The absorbance was recorded in the wavelength range of 230 nm to 1100 nm, and the optical transmission of the films was found to increase for increasing doping concentration of Cu up to 370 nm and then decreased for higher

*Corresponding author: Email: damilola.samson@uniabuja.edu.ng;

wavelengths. ZnO:Cu films displayed high optical transparency which is around 86% - 98% in the visible and infrared regions but minimum in the ultraviolet region. The band gap energy value of the pure ZnO films was found to be 3.20eV, whereas the doped films revealed a continuous decreases for higher doping of Cu concentration, reaching a value of 2.66eV. The refractive index of the films significantly changes with the deposition parameter and increases sharply from 1.4597 to 1.7865 and the highest electrical resistivity was found to be 8.83 $\mu\Omega\text{m}$, and the lowest optical conductivity of 0.113 $\text{M}\Omega\text{m}^{-1}$ was observed in the films with 20% Cu doped film, which indicates that the deposited films are highly suitable for photovoltaic cells and other optoelectronic device applications.

Keywords: ZnO:Cu; spray pyrolysis; electrical properties; optical properties; thin film.

1. INTRODUCTION

Nano-composited materials are generally known for their good structural, optical, and electrical properties performances compared to bulk materials in several applications such as: electronics, biomedical, solar cells, catalysis, and so on. Zinc oxide (ZnO) thin films is one of the most studied group II-VI semiconducting materials that have gained interest and attention of many researchers globally due to its unique properties such as wide direct optical band of about 3.37eV, huge exciton binding energy (~60MeV) at room temperature, high transmission coefficient (>80%) in the visible and near infrared spectra, and high electrical conductivity makes it suitable for possible applications in optoelectronic devices [1-6]. The high ionisation energy and low formation energy of Cu makes it a fast diffusing impurity into ZnO lattice. Cu exhibit both +1 and +2 oxidation states depending on its chemical environment; the role of Cu in ZnO is different from other dopants such as Mn, Co, Bi, Al, Ga, B, In, Y, F, Si, Ge, Ti, Zr, Mg, and As [7]. The radii of Cu^+ (98pm) and Cu^{2+} (80pm) ions are similar to that of Zn^{2+} ion (83pm) [7-8]. Moreover, copper is known as a prominent luminescent activator which enhances the green luminescent band by creating localised states in the band gap of ZnO [9-10]. However, the luminescent and structural properties of Cu doped ZnO nanostructures are affected by different parameters such as growth mechanisms, preheating and post annealing temperatures. The diffusion of Cu into ZnO can cause the formation of complex centres and it is possible that Cu atoms can replace Zn atoms either substitutional or interstitial (Cu) in the ZnO lattice creating structural deformations, thereby affecting the electrical, chemical, structural, morphological and optical properties of ZnO significantly [7]. Several studies have been carried out in recent years on the properties of Cu doped ZnO thin films with various deposition

techniques such as magnetron sputtering, sol-gel coating, spray pyrolysis, pulsed laser deposition (PLD), chemical vapour deposition (CVD), ion plating, atomic layer deposition (ALD), molecular beam epitaxy (MBE), thermal evaporation for HTS deposition, electron beam evaporation [1, 8, 11-17]. Amongst the above mentioned techniques, spray pyrolysis has the advantage of being convenient, simple, cost-effective, flexible and vacuum less processing. It is well suited to control the texture through the tuning deposition parameters such as temperature, rate, thickness, continuous operation and capability for uniform large area coatings. Therefore, a precise study of these properties and their dependence on the film characteristics is very essential as it helps in optimising film parameters for designing of various optoelectronic devices based on Cu doped ZnO nanostructures. In this work, Cu doped ZnO thin films are deposited on microscopic glass substrate by electrostatics spray pyrolysis technique. Copper doping effects on the surface morphological, optical and electrical properties for the prepared thin films are investigated.

2. EXPERIMENTAL DETAILS

2.1 Reagents and Materials

Reagent grade zinc acetate dihydrate [$\text{Zn}(\text{CH}_3\text{COOH})_2 \cdot 2\text{H}_2\text{O}$], copper acetate [$\text{Cu}(\text{CH}_3\text{COO})_2$] and methanol [CH_3OH] were purchased from (99.9% purity, Merck). Ethanol [$\text{C}_2\text{H}_5\text{OH}$], sodium lauryl sulfate [$\text{C}_{12}\text{H}_{25}\text{NaO}_4\text{S}$], and soda lime glass substrates were obtained from (99.9% purity, Sigma-Aldrich). Distilled water of pH 5.5 - 6.5 was used throughout the experiments. All reagents and solvents used in this study were of analytical grade and do not require further purification.

2.2 Sample Preparation and Deposition

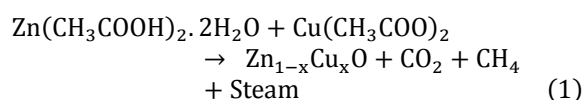
Cu doped ZnO thin films was deposited onto soda lime glass substrates with home-made electrostatic spray pyrolysis system at Namiroch Material Science Laboratory, Abuja, Nigeria. The glass substrates were initially clean and degrease using sodium lauryl, distilled water and ethanol, then allowed to dry in ambient air for 10 min. The cleaned glass substrate was placed onto the substrate heater using the substrate holder. Initially, 0.2 M of zinc acetate solution was prepared by dissolving 4.39 g of zinc acetate in 100 ml of methanol solvent and moderately stirred for 15 min in a sealed glass in order to obtain uniform solution. Further, 0.2M of copper acetate solution was prepared by mixing 3.62 g copper acetate in 100 ml of methanol and stirred continuously for 20 min at room temperature to obtain a homogeneous solution. Additionally, to enhance the solubility of zinc acetate, 0.4 ml of acetic acid was added to the solution and the concentration of the solution was kept at 0.2 M. Five samples were prepared to achieve doping, the precursors were mixed by appropriate volume ratios for doping concentration as coded in Table 1.

Table 1. Sample code, Zn acetate and Cu acetate solutions at different doping concentrations of 0, 5, 10, 15, and 20%

Sample code	Zinc acetate solution (ml)	Copper acetate solution (ml)
CuZnO ₀	10.0	0.0
CuZnO ₅	9.5	0.5
CuZnO ₁₀	9.0	1.0
CuZnO ₁₅	8.5	1.5
CuZnO ₂₀	8.0	2.0

The solutions were then moved into a commercial ultrasonic nebuliser which makes the solutions into aerosol. The aerosol was transported to the substrate by high-purity nitrogen gas and the substrate temperature was kept at 350°C. The clean substrate with a suitable mask were put on the subsector of the heater. The distance between the tip of the nozzle and the surface of the glass substrate were kept constant at 5 cm. Before supplying the compressed air, the substrate temperature was to be kept at a level slightly higher than the required substrate temperature because at the onset of spraying a slight fall of temperature is likely. When compressed air was passed through at a constant pressure of 0.5bar, 0.6ml precursor

volume, 2000µL/hr flow rate and voltage of 5-20 kV, a fine Zn_{1-x}Cu_xO were produced and automatically carried to the reactor zone where film was deposited onto the heated substrate. The deposition time lasted for 15 min and the thickness of the films was about 500 nm to 800 nm. The precursor was then loaded onto the spray pyrolysis deposition system with five different doping concentrations of 0, 5, 10, 15, and 20%. After the deposition, the deposited films were allowed to cool down to room temperature and annealed before being taken out for characterisation. Equation (1) gives the possible chemical reaction in the formation on a substrate of ZnO:Cu thin films:



2.3 Morphological Characterisation of ZnO:Cu Thin Films

Surface morphology of the films and glass substrates, were observed by means of scanning electron microscope (SEM) (EVO I MA10) at an operating voltage of 20kV. The samples were sputter-coated with gold and mounted on carbon tape.

2.4 Optical Characterisation of ZnO:Cu Thin Films

The optical behaviors of the thin films onto glass substrates were investigated using a double beam UV-Vis spectrophotometer (UV-1601, PC Shimadzu) equipped with an integrating sphere accessory for diffuse reflectance. The optical absorption spectra of the film with respect to glass substrate were performed in the wavelength range of 230nm to 1100nm. Measurements were made by placing the samples in the incident beam and another empty glass substrate in the reference beam of the instrument. As the light is transmitted, the sample disrupts the path of the beam, a portion of light was absorbed, a fraction was reflected, or scattered from small particles suspended in the sample, and the rest was transmitted through the sample. The transmission measurements were determine in different parts of the film, scanning the entire sample, and a good reproducibility of the respective samples was generally observed.

2.4.1 Absorbance

The absorption of radiation by any medium occurs through the excitation of electrons and photons. The absorption coefficient (α) of the thin films was estimated in accordance to the Beer-Lambert relation:

$$\alpha \frac{1}{d} \ln \left(\frac{1}{T} \right) \quad (2)$$

Where, d is the film thickness, and T is the measured transmittance.

2.4.2 Transmittance

The transmittance T is calculated from absorbance A by the following formula:

$$T = 10^{(2-A)} \quad (3)$$

If the films are with thickness (d) considerably lower than the thickness of a transparent substrate, the minima (T_{\min}) and maxima (T_{\max}) of the transmission curves can be used as expressed in equations (4) and (5):

$$T_{\min} : nd = \frac{\lambda}{4} (2m + 1) \quad (4)$$

$$T_{\max} : nd = \frac{\lambda}{4} (2m + 2) \quad (5)$$

Where, n is the refractive index of ZnO, λ is the wavelength of the adjacent maxima and minima, and m is the order of the interference minima and maxima ($m = 1, 2, 3, \dots$).

2.4.3 Reflectance

The reflectance (R) of the thin films was determined from the transmittance (T) and absorbance (A) using the relation [18]:

$$R = 1 - T - A \quad (6)$$

2.4.4 Band gap energy

The optical band gap energy is the energy required to move a valence electron into conduction band. Band gap energy (E_g) of ZnO thin films was computed using the extinction coefficient (k) [19-20]:

$$B(E - E_g) = \left[\left(\frac{4\pi k}{\lambda} \right) hv \right]^{\eta/2} \quad (7)$$

Where, B is an energy-independent constant, η is a number that determined the type of the optical transition of the gap materials ($\eta = 1$ for direct gap materials and $\eta = 2$ for an indirect gap materials), h is the plank's constant ($6.626 \times 10^{-34} Js$), ν is the frequency of radiation of light wave, $h\nu$ is the energy of the photon energy, E_g is the optical band gap of valence and conduction band (eV), and λ is the wavelength. Since ZnO is direct band gap semiconductor, hence equation (7) gives:

$$B(E - E_g) = \left[\left(\frac{4\pi k}{\lambda} \right) hv \right]^{1/2} \quad (8)$$

The optical band gap energy (E_g) values for the ZnO thin films are obtained by extrapolating the linear plot of $(\alpha hv)^2$ versus photon energy ($h\nu$) (Tauc's plot) as illustrated in Fig. 5.

2.4.5 Refractive Index

One of the most important optical constants of a material is the refractive index, which in general depends on the wavelength of the electromagnetic wave, through a relationship called dispersion. In materials where an electromagnetic wave can lose its energy during its propagation, the refractive index becomes complex. The real part is usually the refractive index (n), and the imaginary part is called the extinction coefficient (k). The refractive index was calculated from the reflectance (R) using the following relations [19,21-22]:

$$n = \frac{[1 + R] + [2R(2 + k^2) - k^2(1 - R^2)]^{1/2}}{[1 - R]} \quad (9)$$

$$k = \frac{\alpha \lambda}{4\pi} \quad (10)$$

2.5 Electrical Characterisation of ZnO:Cu Thin Films

A QUADPRO-301-6 four-point probe system was used to measure the sheet resistance and the resistivity of the deposited films after which the conductivity was determined from the resistivity. The sheet resistance (R_s) was expressed as:

$$R_s = 4.53 \times \frac{V}{I} \quad (11)$$

Where, V is the measured voltage between the two inner probes and I is the current that passed

through the outer probes. The resistivity was computed from the relation:

$$\rho = R_s \times d_c \quad (12)$$

$$\sigma = \frac{1}{R_s d_c} \quad (13)$$

Where, d_c is the thickness of the conducting layer, ρ is the resistivity, σ is conductivity.

3. RESULTS AND DISCUSSION

3.1 Surface Morphology

The morphological characteristics of undoped ZnO and Cu doped ZnO thin films observed at various percentage doping concentrations of 0, 5, 10, 15 and 20% are shown in Fig. 1 (a-e), which give a general view on the morphology of ZnO thin film deposited on glass substrates.

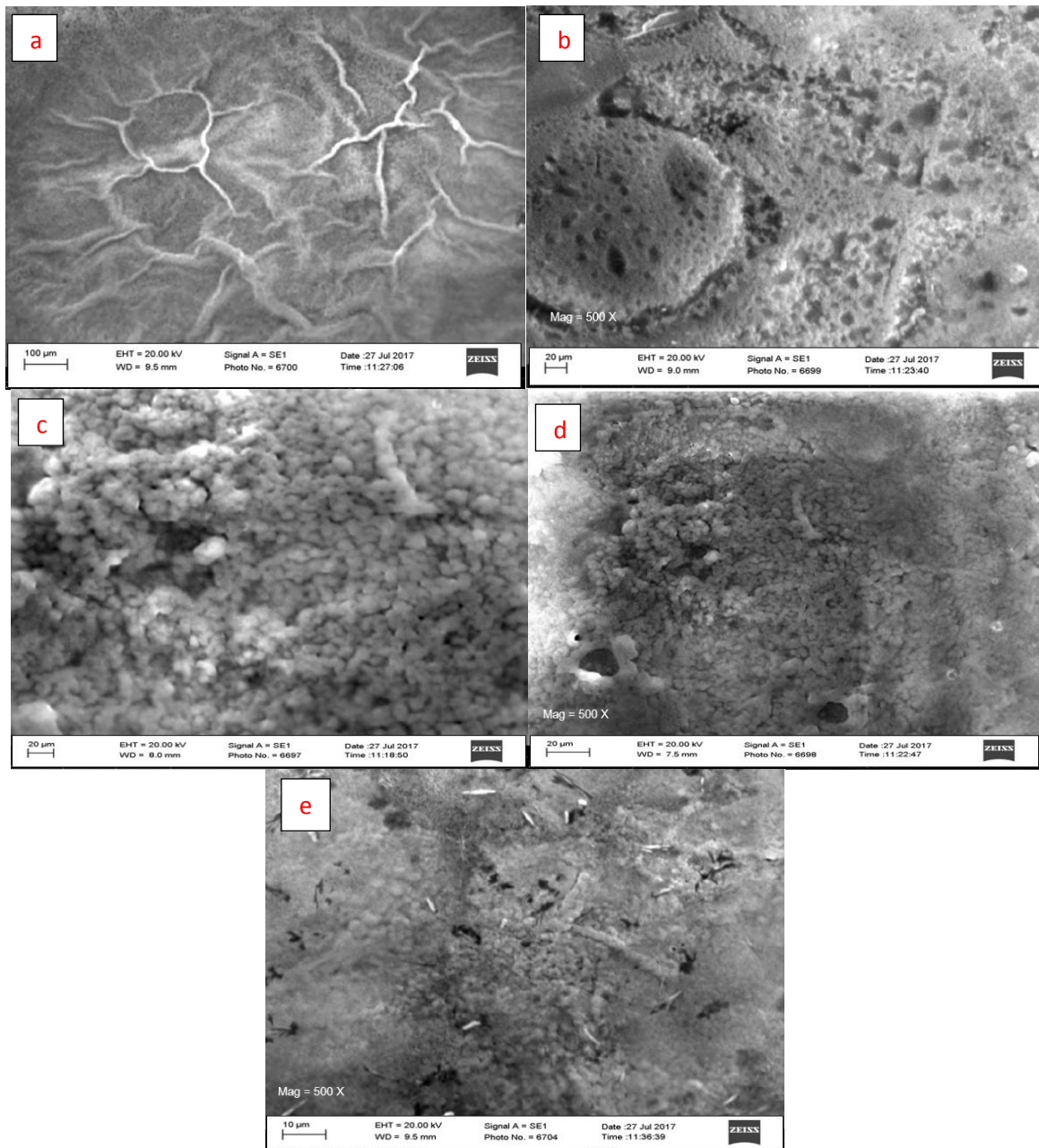


Fig. 1. SEM images of (a) undoped (0%) ZnO; (b) Cu doped ZnO (5%); (c) Cu doped ZnO (10%); (d) Cu doped ZnO (15%); (e) Cu doped ZnO (20%) thin films

The SEM micrographs of the undoped ZnO thin films revealed that the film is uniform and nanofiber structure appear around the nucleation centre of the as-deposited ZnO thin film. The value of the drop on the films surfaces corresponds well with that of drops in aqueous solution of zinc acetate in aerosol. This may be attributed to the formation of ZnO thin films at relatively low substrate temperature of 350°C [14,23]. However, it is clear that copper addition changes the morphology of the particles. Such a variation of the drops morphology reflects the corresponding steps of process evolution during the thermal decomposition of the solution of the precursor. Due to interstitial holes of ZnO filled with copper, most of the fiber were broken and transform into grain as doping concentration increased to 5% (Fig. 1b). After the 5% doping, all the fiber has broken and were transform into grain (Fig. 1c). The size of grain decreases with the increase of Cu up to 15% doping concentration. Interestingly at 20% Cu, a combination of large and small grains were observed (Fig. 1d). This discrepancy in the surface morphologies can be attributed mainly due to the different chemical molar concentration of the precursor solution, growth process and conditions. The diffusion of Cu into ZnO possibly causes the formation of complex centres and likely that Cu atoms are interstitial in the ZnO lattice which create structural deformations, and

thereby affecting the morphological properties of ZnO significantly.

3.2 Optical Properties

Optical properties of pure and Cu doped ZnO thin films such as absorbance, transmittance, reflectance, band gap energy, and refractive index were calculated on as-deposited films in the wavelength range 230 nm to 1100 nm.

3.2.1 Optical absorbance

The UV-Vis spectroscopy optical absorption spectra of undoped ZnO and Cu doped ZnO thin films using different copper doping concentrations are plotted in Fig. 2.

Fig. 2 illustrates the variation of absorbance with wavelength of pure ZnO and Cu doped ZnO thin films. It was observed that the absorbance experience rapid increase at lower wavelengths as the doping concentration level increases. When copper occupies simultaneously both positions within the zinc oxide lattice, the absorbance of ultraviolet light and visible range of the spectra increased. These spectra show high absorbance in the wavelength range from about 313 nm – 452 nm (ultraviolet region) and absorption peaks are found in the ultraviolet

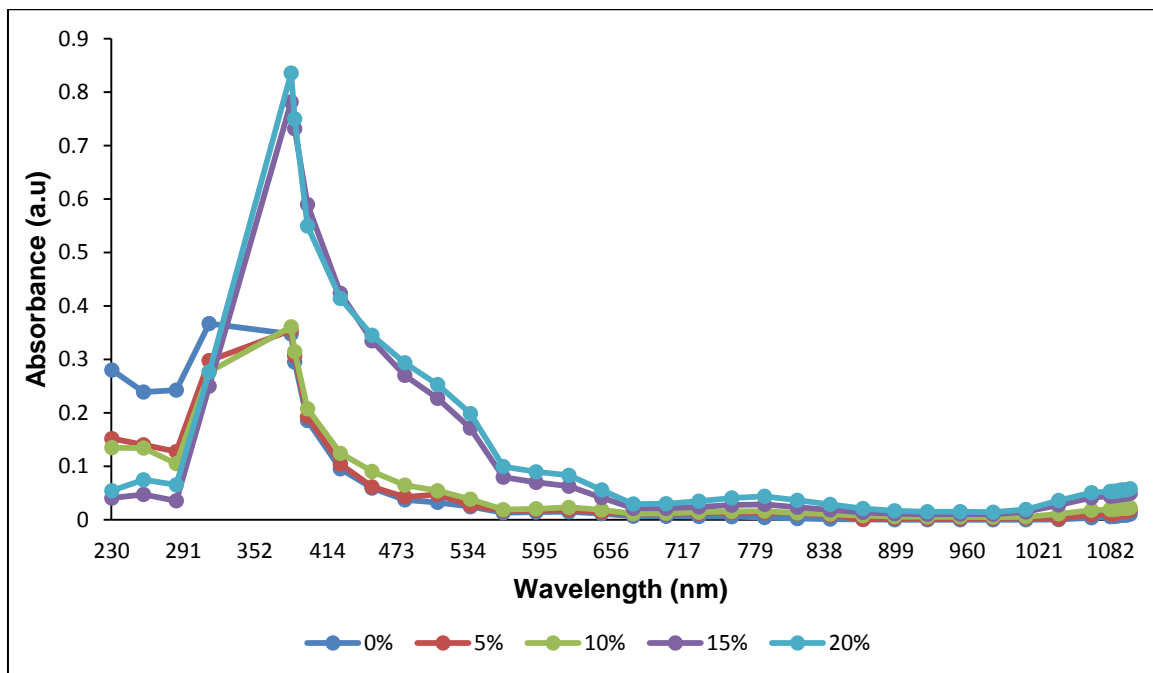


Fig. 2. Variation of absorbance with wavelength of pure ZnO and Cu doped ZnO thin films at 0, 5, 10, 15, and 20%

region near the wavelength 383nm but very low at the visible and infrared regions of solar spectra because of higher transmittance of the films in this region. This revealed that, beyond the band edge the absorbance is very small and the transmittance is high, which illustrates that the obtained thin films are of low impurities. The reduction of absorbance in Cu doped samples for higher wavelengths can be explained as due to the removal of defects and disorder in the as-deposited film by Cu doping. The intensity of these absorption bands also increases with the increase in copper concentration which confirms the consistent incorporation of the Cu^{2+} into ZnO lattice. Moreover, as the Cu doping concentration increase up to 20%, the intensity of the absorption bands decreases as a result of the formation of ZnCu_2O_4 spinel phase, causing a limits of the solubility of copper into zinc oxide. This attribution of absorbance mainly depends upon some of the factors like particle size, thickness, oxygen deficiency, and lattice strain etc.

3.2.2 Optical transmittance

The UV-Vis transmission spectra of the thin films have been observed in the wavelength range from 230nm to 1100nm and are presented in Fig. 3.

The plot of optical transmittance of pure ZnO and Cu doped ZnO thin films with different Cu

concentrations as indicated in Fig. 3 reveals that the values of transmittance decreases sharply with increasing wavelength near the ultraviolet region reaching a minimum at wavelength (~383nm) due to the band gap absorption. The transmittance then increases with respect to film thickness for wavelength up to 700nm after which it is relatively constant. The undoped ZnO thin films showed high transparency in the visible region. The average value of the optical transmittance of undoped ZnO and ZnO:Cu films lies in the range 86% - 98% with a shape fundamental absorption edge. The entire transmittance spectra reveals steep absorbance edges at the wavelength range of 313nm to 385nm indicative of good crystalline nature of ZnO:Cu with low defect density attractive for optoelectronic and solar cell applications [24-25]. The flat aspect of the transmission curve without interference fringes emphasises the surface homogeneity with small crystallite size. Furthermore, the transmittance indicates oscillations caused by interference as a result of good film crystallinity and surface smoothness. The loss of transmittance may be attributed to the incorporation of Cu^{2+} ions which replaces the substitutional or interstitial Zn^{2+} ions from the host lattice. This incorporation of Cu^{2+} ions produces stresses in the films which causes the structural deformation or defects in the thin films. This will in turn increase the photon scattering from the defects [26]. For higher doping levels, the samples were from

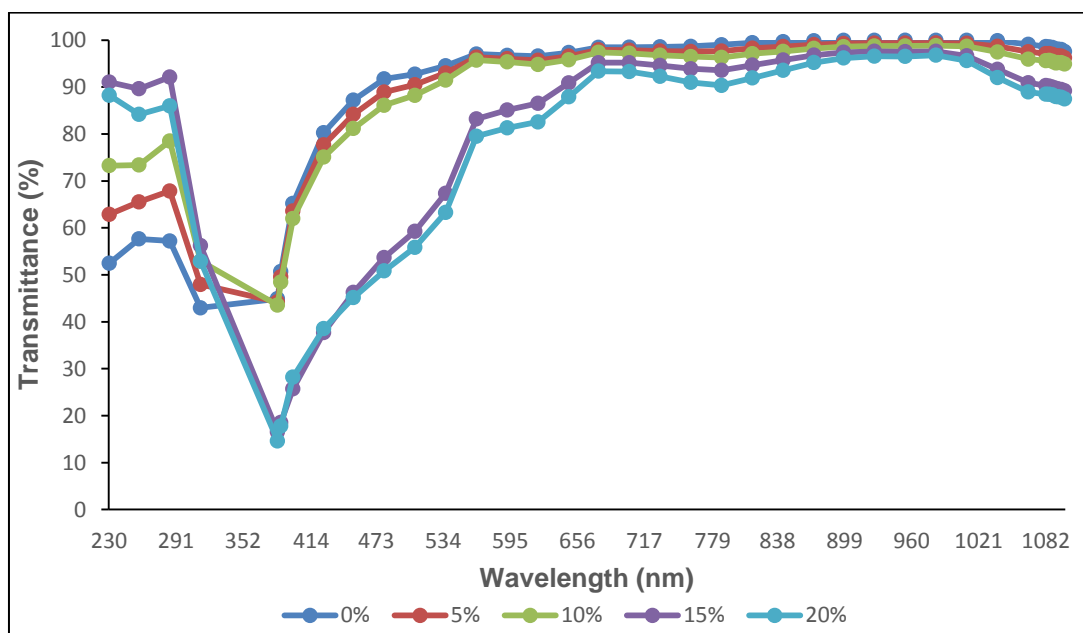


Fig. 3. Variation of optical transmittance with wavelength of pure and Cu doped ZnO thin films at 0, 5, 10, 15, and 20%

light to deep silvery in colour and less transparent to naked eye. The changes in the transmittance and absorption edge wavelength of ZnO thin films can be imputed to the difference in surface morphologies, phase structure, crystallite size, and compositions within the thin films.

3.2.3 Optical reflectance

Diffuse reflectance spectra were recorded to estimate the optical band gap of the pure ZnO and Cu doped ZnO with different concentrations. Fig. 4 indicate the extrapolation of the diffuse reflectance absorption spectra with wavelength curve of the pure ZnO and Cu doped ZnO thin films.

It is observed that the absorption slightly decreases as the wavelength increases and broaden significantly into the visible region, with 20% Cu doping concentration showing large scattering component. The reflectance increases with increasing doping concentration level in the wavelength range of 313 nm to 560 nm, then decreased as the wavelength increases. Also, it was revealed that the samples become more silverer in color as the level of doping increases, which is a visual manifestation of decrease diffuse reflectance spectra with increasing level

of doping concentrations of copper. The copper doping causes little structural disorder in ZnO lattice.

3.2.5 Optical band gap energy

The optical band gap energy (E_g) of pure ZnO and Cu doped ZnO thin films have been observed in the wavelength range from 230nm to 1100nm as presented in Fig. 5 (a-e).

The E_g values of the thin films are found between 2.66eV and 3.20eV, with the pure ZnO exhibit highest optical band gap energy and red shift as a consequence of exciton confinement due to decreased grain size. The decrease in the optical band gap energy is as a result of the increase in copper doping concentration, thickness, which also induces crystallinity. Similar results of decrease in band gap have also been reported on Cu doped ZnO thin films deposited onto glass substrate by spray pyrolysis techniques [27-28]. The optical band gap of ZnO decreased by 0.54eV due to copper doping, this is as a result of lower band gap values of copper oxides [28]. Furthermore, hybridisation of the copper 3d bands with oxygen 2p bands leads to an exchange interaction and big crystallite size that decreases the band gap of Cu doped ZnO.

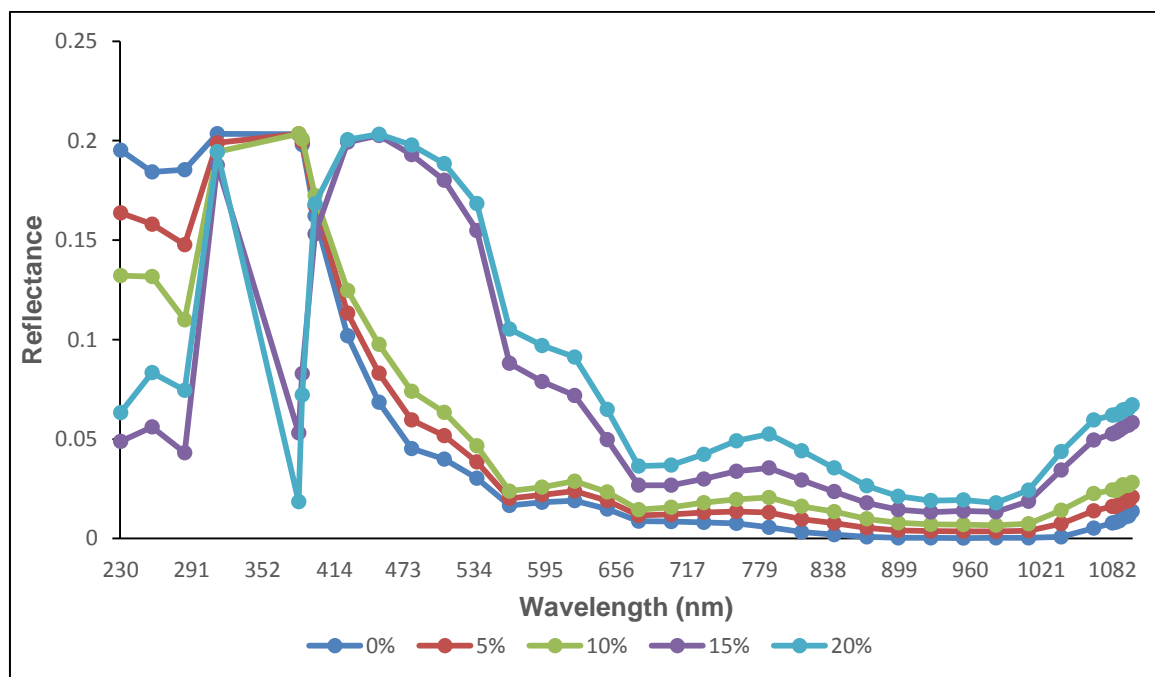


Fig. 4. Variation of diffuse reflectance spectra with wavelength of pure ZnO and Cu doped ZnO thin films at 0, 5, 10, 15, and 20%

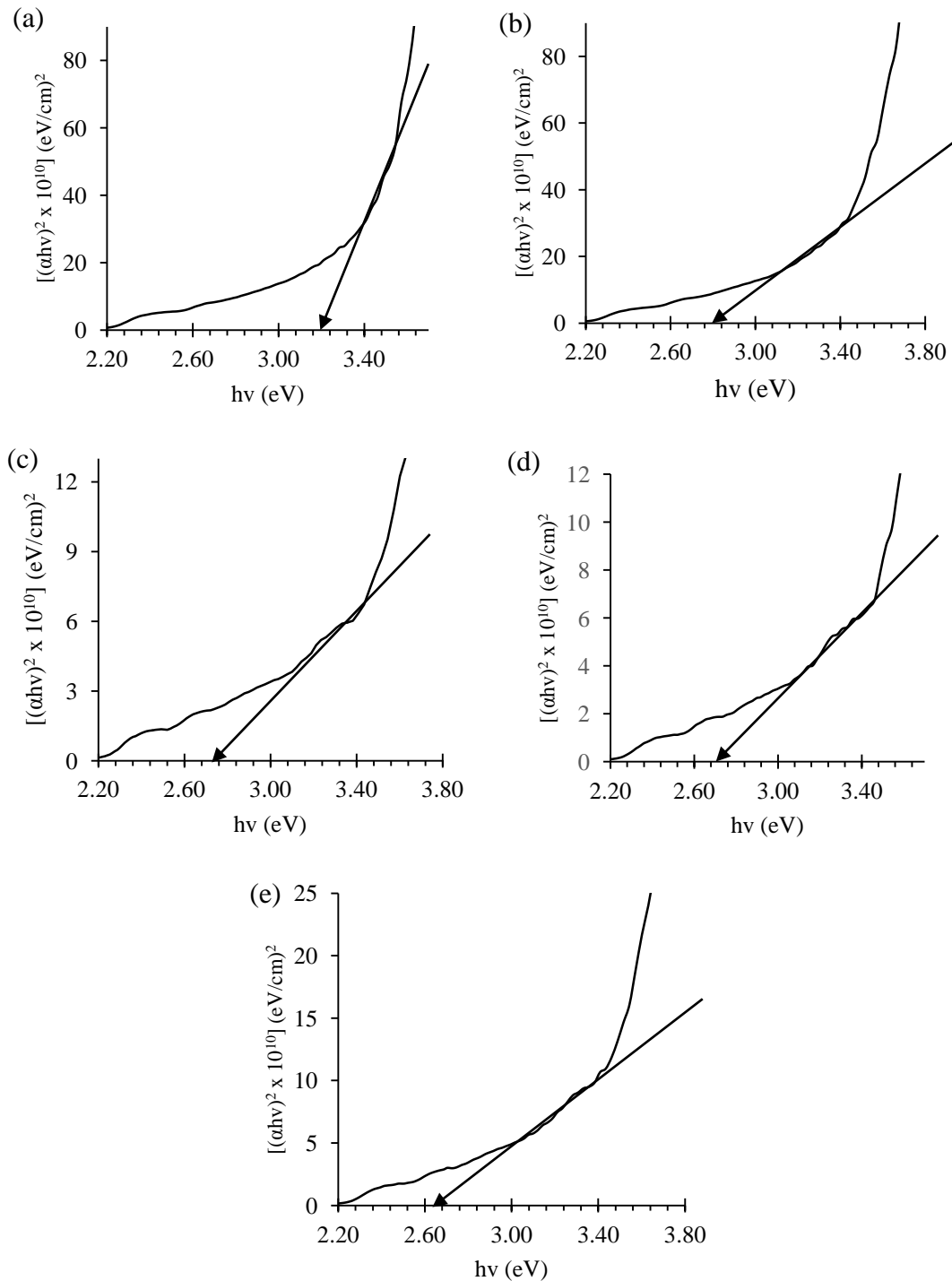


Fig. 5. Tauc plots indicating the variation of the optical band gap energy of pure ZnO and Cu doped ZnO thin films as a function of the incident photon energy deposited at (a) 0 (b) 5, (c) 10, (d) 15 and (e) 20%

3.2.4 Refractive index

The refractive index of the films has been calculated from the diffuse reflectance spectra using equation (9). The results are

shown in Table 2 and with a graphical illustration in Fig. 6.

The refractive index of the thin films significantly change with the deposition parameter. It shows

that the refractive index increases when films transmittance increases with increasing Cu doping concentration. The refractive index of undoped ZnO film is significantly lower as compared to other samples, probably due to the presence of organic residues that are not completely removed from the film.

3.3 Electrical Properties

3.3.1 Resistivity

The electrical resistivity of pure ZnO and Cu doped ZnO thin films have been measured by four-probe techniques as shown in Fig. 7.

Fig. 7 shows that the electrical resistivity increases upon increasing the doping concentration level which may be due to the increased solubility limit of Cu in the ZnO structure [29]. The least electrical resistivity were observed at 0% while 20% Cu doped film recorded the highest electrical resistivity, due to the chemisorption of oxygen at grain boundaries which is possible since the carrier gas used during deposition was ambient air. The three co-ordinated Zn, Cu and Cu cations have ionic radii

of 0.06, 0.06 and 0.057nm respectively, with stable electronic configuration, Zn^{2+} ($3d^{10}$), Cu^{2+} ($3d^9$) and Cu^+ ($3d^{10}$). Diffusion at high firing temperature may lead to a defect reactions in which Cu^{2+} cations substitute Zn^{2+} cations in the wurtzite unit cell of ZnO. The stability of the coulomb forces of the interactions between the acceptor defect and intrinsic ZnO donors might be due to the capture of an electron from the lattice.

3.3.2 Conductivity

The variations of electrical conductivity with temperature for as-deposited pure ZnO and Cu:ZnO thin films are presented in Fig. 8.

Table 2. Average refractive indices of pure ZnO and Cu doped ZnO at various concentrations of 0, 5, 10, 15, and 20%

Sample code	Refractive index (n)
CuZnO ₀	1.4597
CuZnO ₅	1.5032
CuZnO ₁₀	1.5405
CuZnO ₁₅	1.6996
CuZnO ₂₀	1.7865

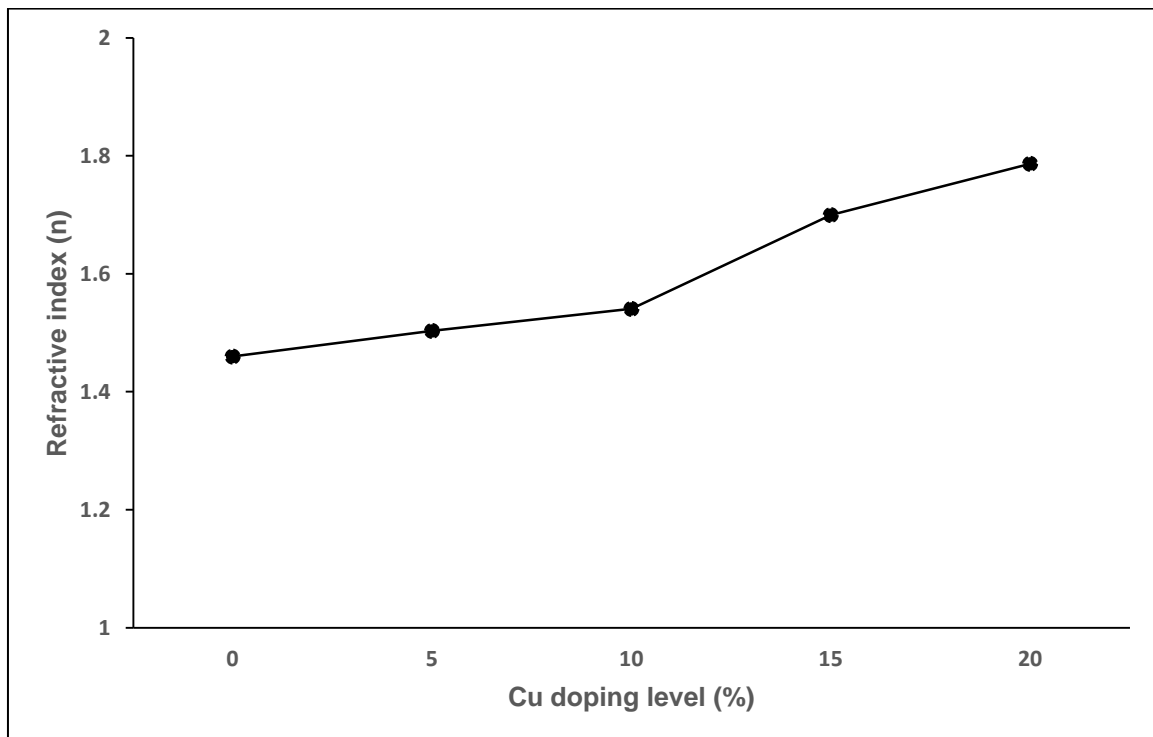


Fig. 6. Variation of refractive indices of pure ZnO and Cu doped ZnO thin films at 0, 5, 10, 15, and 20% concentrations

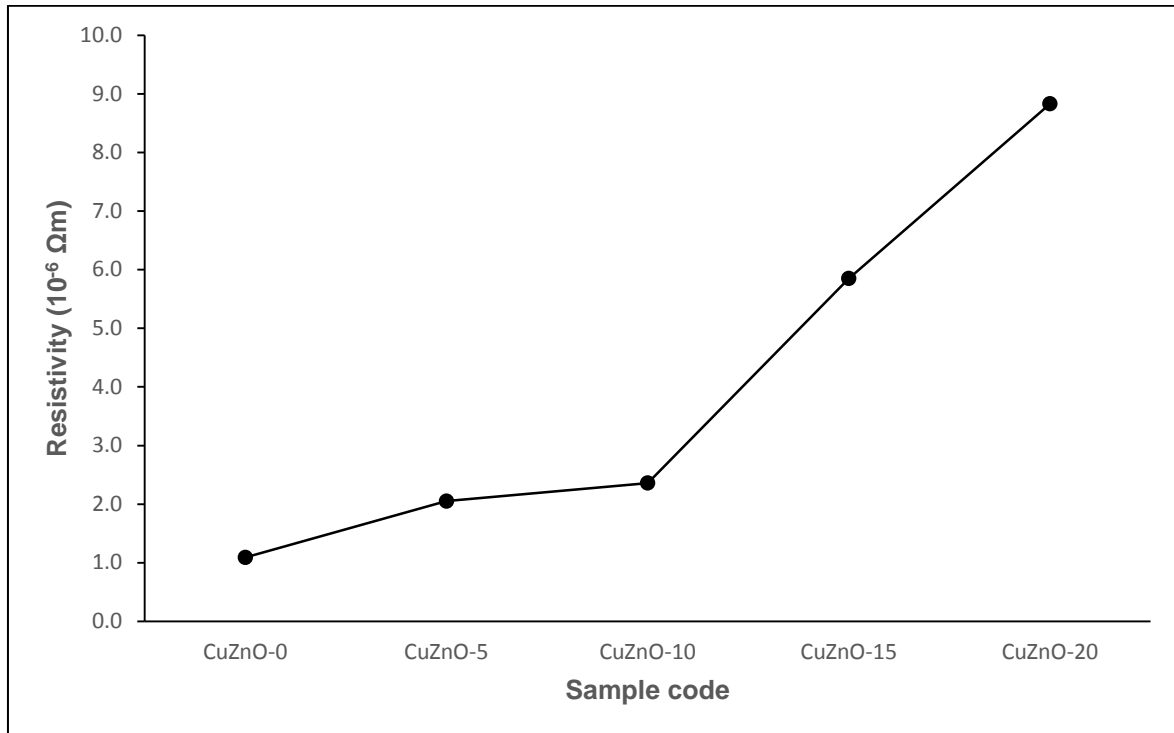


Fig. 7. Resistivity of pure ZnO and composite Cu:ZnO thin films with various concentrations

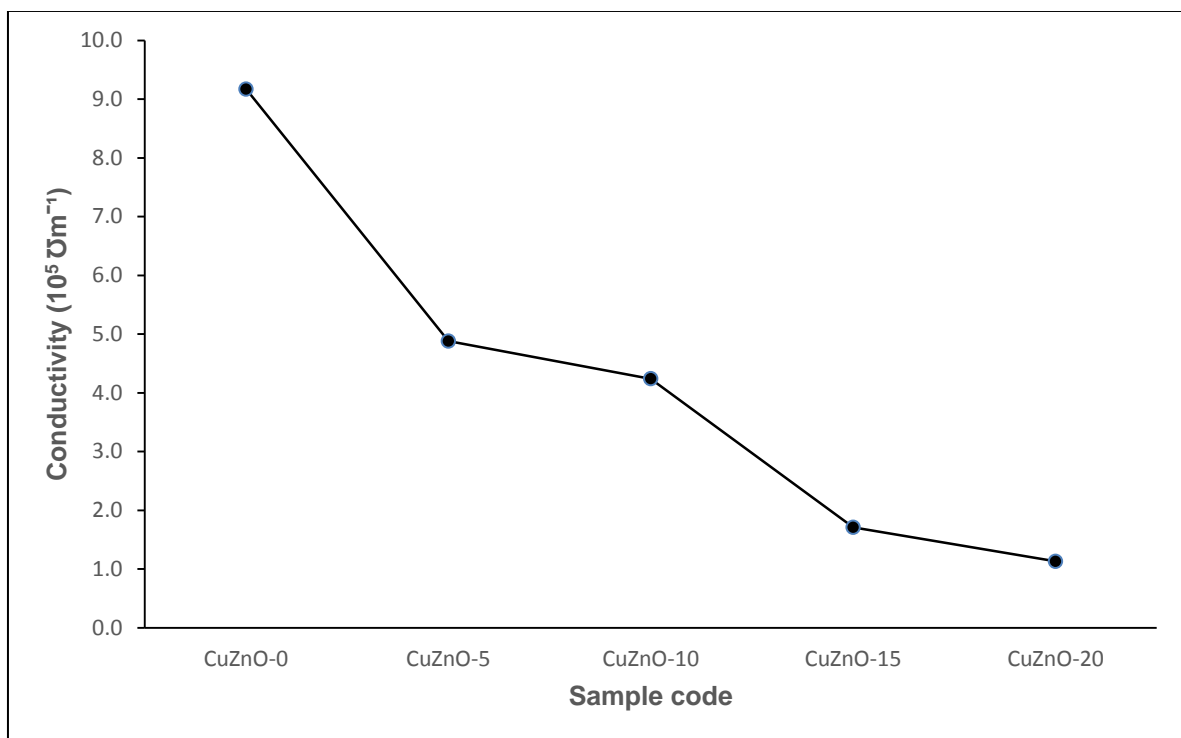


Fig. 8. Conductivity of pure ZnO and composite Cu:ZnO thin films with various concentrations

This type of variation indicates the semiconducting behavior of the films. The electrical conductivity decreases with increase in ZnO films concentration. Electrical conductivity of ZnO depend not only on the concentration of the carriers but also on their mobility. Incorporation

of Cu into ZnO reduces its conductivity as Cu introduces deep acceptor level and it traps electrons from the conduction band.

4. CONCLUSION

In this work, Cu ion was successively doped into ZnO lattice using the electrostatic spray pyrolysis technique at the substrate temperature of 350°C. SEM micrographs show that all the films are found well covered on the glass substrate and sprayed particles are well adhered to the glass substrates. Due to interstitial, holes of ZnO are filled with Cu, most of the fiber broke and transformed into grain at 5% Cu. The size of grain decreases with the increase of Cu in 15%, but at 20% Cu, a combination of large and small grains were observed. These spectra show high absorbance in the wavelength range from about 313 nm – 452 nm (ultraviolet region) and absorption peaks are found in the ultraviolet region near the wavelength 383 nm but very low at the visible and infrared regions of solar spectra because of higher transmittance of the films in this region. The results revealed that all the films deposited have high transmittance values in the range of 86% to 98% in the visible and infrared regions but minimum in the ultraviolet region. It was observed that the absorption slightly decreases as the wavelength increases and extends significantly into the visible region, with 20% showing large scattering component. ZnCu₂O₄ spinel phase appears above the solubility limit, which affects the optical and electrical properties of Cu doped ZnO thin films. The band gap energy value of the pure ZnO films was found to be 3.20eV, whereas the doped films revealed a continuous decreases for higher doping of Cu concentration, reaching a value of 2.66eV. The refractive index increases sharply from 1.4597 to 1.7865 as Cu doping content increases. The electrical resistivity of ZnO:Cu films (20%) increases as a result of the chemisorption of oxygen at grain boundaries which is due to the carrier gas used during deposition. The optical conductivity was found to decrease with the increase in Cu addition and this might be due to the deep acceptor level and traps electrons from the conduction band. The present work shows that by controlling the particle size, it is possible to attain almost 99% transmission in the visible range. The achieved parameters are more suitable for developing photovoltaic cells and other optoelectronic device because the films have less than 40% transmittance in the UV region.

ACKNOWLEDGEMENTS

We acknowledge the support of the laboratory staff of Namiroch Material Science Laboratory, Abuja, Nigeria for this work.

COMPETING INTERESTS

Authors have declared that no competing interests exist.

REFERENCES

1. Andrzej M, Piotr S, Marian K, Volodymyr P. Zinc oxide films prepared by spray pyrolysis. EPJ Web of Conferences. 2017; 133:03004. DOI: 10.1051/epjconf/201713303004
2. Rusu DI, Rusu GG, Luca D. Structural characteristics and optical properties of thermally oxidized zinc films. Acta Physica Polonica A. 2011;119(6):850-856.
3. Tewari S, Bhattacharjee A. Structural, electrical and optical studies on spray-deposited aluminum-doped ZnO thin films. PRAMANA Journal of physics. 2011;76(1): 153-63.
4. Kim JY, Jeong H, Jang DJ. Hydrothermal fabrication of well-ordered Zn Onanowire arrays on Zn foil: Room temperature ultraviolet nanolasers. Journal of Nanoparticle Research. 2011;13: 6699-6706.
5. Liu X, Jin Z, Bu S, Zhao J, Liu Z. Effect of buffer layer on solution deposited ZnO films. Materials Letters. 2005;59(29-30): 3994-3999.
6. Hu YH, Chen YC, Xu HJ, Gao H, Jiang WH, Hu F, Wang YX. Texture ZnO thin films and their application as front electrode in solar cells. 2010;973-978. DOI: 10.4236/eng.2010.212124
7. Behera D, Panigrahi J, Acharya BS. Probing the effect of nitrogen gas on electrical conduction phenomena of ZnO and Cu-doped ZnO thin films prepared by spray pyrolysis. Ionics. 2011;17:741–749. DOI: 10.1007/s11581-011-0564-0
8. Rahmani MB, Keshmiri SH, Shafiei M, Latham K, Wlodarski W, Plessis J, Zadeh KK. Transition from n- to p-type of spray pyrolysis deposited Cu doped ZnO thin films for NO₂ sensing. Sensor Letters. 2009;7:1-8.

9. Buchholz D, Chang R, Song J, Ketterson J. Room temperature ferromagnetism in Cu-doped ZnO thin films. *Applied Physics Letters*. 2005;87(8):082504-082504.
10. Chakraborti D, Narayan J, Prater J. Room temperature ferromagnetism in Zn_{1-x}Cu_xO thin films. *Applied Physics Letters*. 2007;90(6):062504-062504.
11. Sahay PP, Tewari S, Nath RK. Optical and electrical studies on spray deposited ZnO thin films. *Cryst. Res. Technol.* 2007;42(7): 723-729.
12. Tan T, Li Y, Liu Y. Two-step preparation of Ag/tetrapod-like ZnO with photocatalytic activity by thermal evaporation and sputtering. *Material Chemistry Physics*. 2008;111:305-308.
13. Chen LC, Hsieh CA, Zhang X. Electrical properties of CZO films prepared by ultrasonic spray pyrolysis. *Materials*. 2014;7:7304-7313.
DOI: 10.3390/ma7117304
14. Islam MR, Podder J. Optical properties of ZnO nano fiber thin films grows by spray pyrolysis of zinc acetate precursor. *Crystallography Research and Technology*. 2009;44(3):286-292.
15. Horzum S, Torun E, Serin T, Peeters FM. Structural, electronic and optical properties of Cu-doped ZnO: Experimental and theoretical investigation. *Philosophical Magazine*. 2016;96(17):1743-1756.
DOI: 10.1080/14786435.2016.1177224
16. Thakur S, Sharma N, Varkia A, Kumar A. Structural and optical properties of copper doped ZnO nanoparticles and thin films. *Advances in Applied Science Research*. 2014;5(4):18-24.
17. Ueda K, Tabata H, Kawai T. Magnetic and electrical properties of transition-metal-doped ZnO films. *Applied Physical Letters*. 2001;79(7):988-990.
18. Offor PO, Okorie BA, Lokhande CD, Patil PS, Ezema FI, Omah AD, Aigbodion VS, Ezekoye BA, Ezema IC. The properties of spray-deposited zinc sulfide thin films using trisodium citrate complexant. *Int. J Adv Manuf Technol*. 2018;95:1849-1857.
Available:<https://doi.org/10.1007/s00170-017-1326-6>
19. Ganesh V, Shkir M, AlFaify S, Yahia IS, Zahran HY, El-Rehim AFA. Study on structural, linear and nonlinear optical properties of spin coated N doped CdO thin films for optoelectronic applications. *J. Mol. Struct.* 2017;1150:523-530.
20. Ray SC. Preparation of copper oxide thin films by the sol-gel like dip technique and study of their structural and optical properties. *Sol. Energy Mater. Sol. Cells*. 2001;68:307-312.
21. Shkir M, Ganesh V, AlFaify S, Yahia IS. Structural, linear and third order non-linear optical properties of drop casting deposited high quality nanocrystalline phenol red thin films. *J. Mater. Sci. Mater. Electron*. 2017; 28:10573-10581.
22. You ZZ, Hua GJ. Electrical, optical and microstructure properties of transparent conducting GZO thin films deposited by magnetron sputtering. *J. Alloys Comp.* 2012;530:11-17.
23. Llicana S, Caglara M, Yakuphanoglu F. Electrical conductivity, optical and structural properties of indium-doped ZnO nanofiber thin film deposited by spray pyrolysis method. *Physica E*. 2006; 35(131).
24. Deva Arun Kumar K, Valanarasu S, Tamilnayagam V, Amalraj L. Structural, morphological and optical properties of SnS₂ thin films by nebulized spray pyrolysis technique. *J Mater Sci: Mater Electron*. 2017;28:14209-14216.
DOI:10.1007/s10854-017-7278-7.
25. Ravichandran K, Mohan R, Begum NJ, Snega S, Swaminathan K, Ravidhas C, Sakthivel B, Varadharajaperumal S. Impact of spray flux density and vacuum annealing on the transparent conducting properties of doubly doped (Sn + F) zinc oxide films deposited using a simplified spray technique. *Vacuum*. 2014;107:68-76.
26. Znaidi L. Sol-gel deposited ZnO thin films: A review. *Materials Science and Engineering: B*. 2010;174(1):18-30.
27. Mani GK, Rayappan J. Influence of copper doping on structural, optical and sensing properties of spray deposited zinc oxide thin films. *J. Alloys Compd.* 2014;582:414-419.
28. Tarwal NL, Gurav KV, Mujawar SH, Sadale SB, Nam KW, Bae WR, Moholkar AV, Kim JH, Patil PS, Jang JH. Photoluminescence and photoelectrochemical properties of the spray deposited copper doped zinc oxide thin films. *Ceram. Int.* 2014;40:7669-7677.

29. Ravichandran K, Dineshbabu N, Arun T, Ravidhas C, Valanarasu S. Effect of fluorine (an anionic dopant) on transparent conducting properties of Sb (a cationic) doped ZnO thin films deposited using a simplified spray technique. Mater. Res. Bull. 2016;83:442-452.

© 2018 Samson and Makama; This is an Open Access article distributed under the terms of the Creative Commons Attribution License (<http://creativecommons.org/licenses/by/4.0>), which permits unrestricted use, distribution, and reproduction in any medium, provided the original work is properly cited.

Peer-review history:

The peer review history for this paper can be accessed here:

<http://www.sciencedomain.org/review-history/27355>